Institute for Mathematics and its Applications
University of Minnesota
400 Lind Hall, 207 Church St. SE, Minneapolis, MN 55455

Numerical Simulation and Control of Sublimation Growth of SiC Bulk Single Crystals: Modeling, Finite Volume Method, Analysis and Results

Peter Philip

Applied Mathematics and Numerical Analysis Seminar
School of Mathematics, University of Minnesota
September 16, 2004

Joint work with:

- Jürgen Geiser, Olaf Klein, Jürgen Sprekels, Krzysztof Wilmański
  (Weierstrass Institute for Applied Analysis and Stochastics (WIAS), Berlin)
  (modeling, finite volume method)

- Christian Meyer, Fredi Tröltzsch
  (TU Berlin, Department of Mathematics) (optimal control)

Cooperation with:

- Klaus Böttcher, Detev Schulz, Dietmar Siche
  (Institute of Crystal Growth (IKZ), Berlin) (growth experiments)

Supported by:

- Research Center "Matheon: Mathematics for Key Technologies" of the German Science Foundation (DFG) (2002 – 2004)

- German Ministry for Education and Research (BMBF) (1997 – 2002)

Overview

- SiC bulk single crystals: applications and growth process
- Modeling: balance equations, radiative heat transfer, induction heating
- Discretization: finite volume method
- Numerical simulation: software WIAS-HiTNIHS, transient simulation results
- Optimal control: theoretical results, numerical results

Publications / More Information:

`http://www.ima.umn.edu/~philip/sic/#Publications`

`http://www.ima.umn.edu/~philip/sic/`

Overview

- SiC bulk single crystals: applications and growth process
- Modeling: balance equations, radiative heat transfer, induction heating
- Discretization: finite volume method
- Numerical simulation: software WIAS-HiTNIHS, transient simulation results
- Optimal control: theoretical results, numerical results

Publications / More Information:

`http://www.ima.umn.edu/~philip/sic/#Publications`

`http://www.ima.umn.edu/~philip/sic/`

Applications of SiC bulk single crystals

Light-emitting diodes:
Lifetime: $\approx$ 10 years
Light extraction efficiency $>$ 32 %
(light bulb: $\approx$ 10 %)

Blue laser:
Its application in the DVD player
admits up to 10-fold capacity of disc

SiC-based electronics still works
at 600 deg. Celsius,
SiC sensors placed close to car
engines can save resources and costs

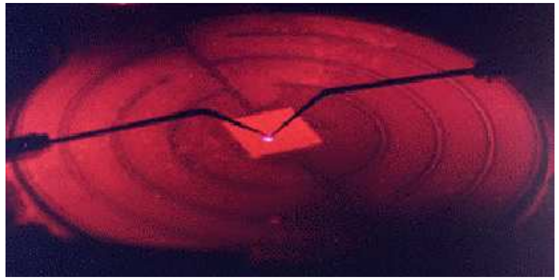

SiC growth by physical vapor transport (PVT)

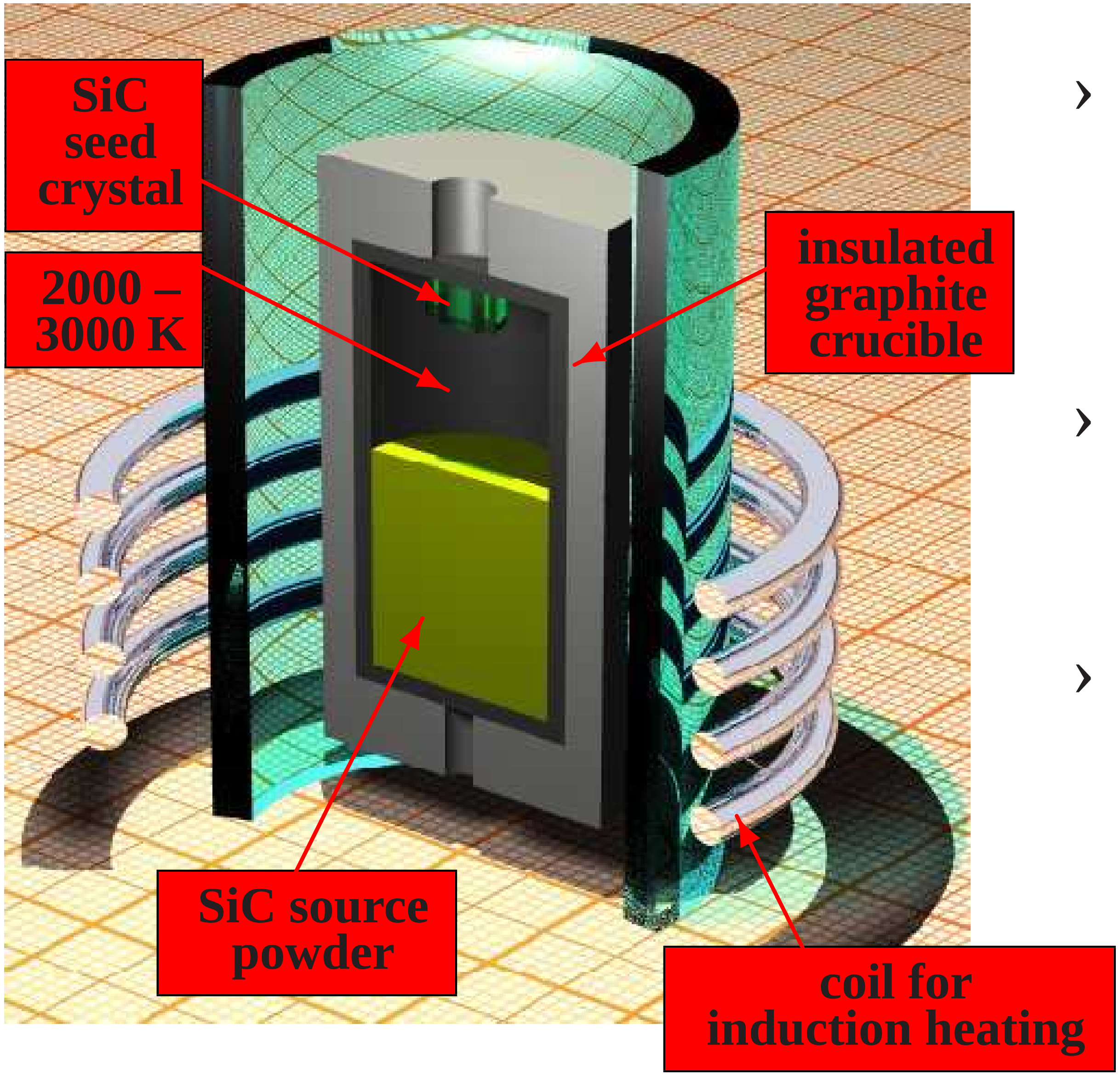

- polycrystalline SiC powder sublimates inside induction-heated graphite crucible at 2000 – 3000 K and $\approx$ 20 hPa
- a gas mixture consisting of Ar (inert gas), Si, SiC_2, Si_2C, . . . is created
- an SiC single crystal grows on a cooled seed

Problems:

- Needed: Perfect single crystals as large and as quick as possible (currently: ∅ 5 – 10 cm, one growth run: 2 – 3 days)

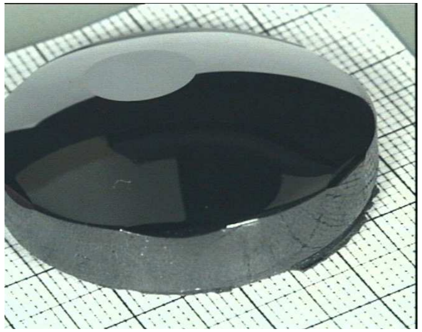

- High energy costs, high costs for apparatus replacement (every 10 runs)
- Wrong control parameters (setup, position of induction coil, heating power) ⇒ (costly !) failure of growth run

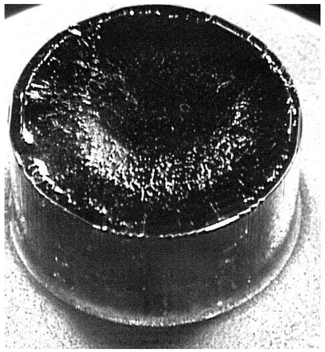

- High temperatures prevent measurements inside growth apparatus ⇒ experimental optimization of process is difficult and costly

Goal:

Stationary and transient optimal control of process, using mathematical modeling, numerical simulation.

Overview

- SiC bulk single crystals: applications and growth process
- Modeling: balance equations, radiative heat transfer, induction heating
- Discretization: finite volume method
- Numerical simulation: software WIAS-HiTNIHS, transient simulation results
- Optimal control: theoretical results, numerical results

Model includes

1. Heat conduction in gas, graphite, powder, crystal
2. Radiative heat transfer between cavities (nonlocal integral operators)
3. Semi-transparency of crystal (band model)
4. Induction heating (Maxwell's equations)
5. Mass transport in gas, powder, graphite (Euler equations, porous media equations, . . .)
6. Chemical reactions in gas (reaction-diffusion equations)
7. Crystal growth, sublimation of source powder, decomposition of graphite walls (multiple free boundaries)

Model of the gas phase

Continuous mixture theory and material laws (ideal gas etc.) yield:

- Mass balance:

$$\frac{\partial \rho_{\mathrm{gas}}}{\partial t} + \mathrm{div}\left(\rho_{\mathrm{gas}} \mathbf{v}_{\mathrm{gas}}\right) = 0. \tag{1a}$$

- Momentum balance:

$$\frac{\partial \left(\rho_{\mathrm{gas}} \mathbf{v}_{\mathrm{gas}}\right)}{\partial t} + \mathrm{div}\left(p_{\mathrm{gas}} \mathbf{1}\right) = \rho_{\mathrm{gas}} \mathbf{g}, \tag{1b}$$

$$p_{\mathrm{gas}} = R\, \rho_{\mathrm{gas}}\, T_{\mathrm{gas}} \sum_{\iota=1}^{A} \frac{c^{(\alpha_\iota)}}{M^{(\alpha_\iota)}}.$$

t: time, R: universal gas constant, $\mathbf{g}$: gravimetric acceleration.

Quantities in the gas mixture:

ρ_{gas}: mass density, $\mathbf{v}_{\mathrm{gas}}$: local mean velocity, p_{gas}: pressure, T_{gas}: absolute temperature.

Quantities in the gas component α_ι:

$c^{(\alpha_\iota)}$: concentration, $M^{(\alpha_\iota)}$: molecular mass.

› Energy balance:

$$\frac{\partial}{\partial t}\left(\rho_{\mathrm{gas}}\varepsilon_{\mathrm{gas}}\right)+\operatorname{div}\left(\rho_{\mathrm{gas}}\varepsilon_{\mathrm{gas}}\mathbf{v}_{\mathrm{gas}}+\mathbf{q}_{\mathrm{gas}}+p_{\mathrm{gas}}\mathbf{v}_{\mathrm{gas}}\right)=\rho_{\mathrm{gas}}\mathbf{g}\bullet\mathbf{v}_{\mathrm{gas}}, \tag{1c}$$

$$\begin{aligned}
\varepsilon_{\mathrm{gas}} &= R\,T_{\mathrm{gas}}\sum_{\iota=1}^{A} z^{(\alpha_\iota)}\frac{c^{(\alpha_\iota)}}{M^{(\alpha_\iota)}},\\
\mathbf{q}_{\mathrm{gas}} &= -\kappa_{\mathrm{gas}}\,\nabla\,T_{\mathrm{gas}}\\
&\quad - R^2\,\rho_{\mathrm{gas}}\,T_{\mathrm{gas}}\sum_{\iota=1}^{A}\frac{c^{(\alpha_\iota)}\left(z^{(\alpha_\iota)}+1\right)}{\left(M^{(\alpha_\iota)}\right)^2}\cdot\left(D^{(\alpha_\iota)}\right)^{-1}\nabla\left(\rho_{\mathrm{gas}}c^{(\alpha_\iota)}\,T_{\mathrm{gas}}\right)\\
&\quad + R^2\,\rho_{\mathrm{gas}}\,T_{\mathrm{gas}}\sum_{\iota,\iota'=1}^{A}\frac{\left(c^{(\alpha_\iota)}\right)^2\left(z^{(\alpha_\iota)}+1\right)}{M^{(\alpha_\iota)}M^{(\alpha_{\iota'})}}\cdot\left(D^{(\alpha_\iota)}\right)^{-1}\nabla\left(\rho_{\mathrm{gas}}\,T_{\mathrm{gas}}c^{(\alpha_{\iota'})}\right).
\end{aligned}$$

Quantities in the gas mixture:

$\varepsilon_{\mathrm{gas}}$: internal energy, $\mathbf{q}_{\mathrm{gas}}$: heat flux, κ_{gas}: thermal conductivity.

Quantities in the gas component α_ι:

$z^{(\alpha_\iota)}$: configuration number, $D^{(\alpha_\iota)}$: diffusion coefficient.

- Reaction-diffusion equations ($\iota \in \{1, \dots, A\}$):

$$\frac{d\,c^{(\alpha_\iota)}}{dt} - \frac{1}{\rho_{\text{gas}}}\,\text{div}\left(\rho_{\text{gas}} c^{(\alpha_\iota)} \left(D^{(\alpha_\iota)}\right)^{-1} \cdot \left(\nabla\,\rho_{\text{gas}} c^{(\alpha_\iota)} \frac{R}{M^{(\alpha_\iota)}} T_{\text{gas}} - c^{(\alpha_\iota)}\,\nabla\,p_{\text{gas}}\right)\right) = \frac{1}{\rho_{\text{gas}}} \sum_{a=1}^{n} \gamma_a^{(\alpha_\iota)} M^{(\alpha_\iota)} M^{(\text{H})} \Lambda_a. \tag{1d}$$

$\gamma_a^{(\alpha_\iota)}$: stoichiometric coefficients,

H: hydrogen,

Λ_a: rates of chemical reactions and phase transitions.

Nonlinear heat conduction in solid material β_j, $j \in \{1, \ldots, N\}$

$$\rho^{[\beta_j]} c_{\mathrm{sp}}^{[\beta_j]} \frac{\partial T^{[\beta_j]}}{\partial t} + \operatorname{div} \mathbf{q}^{[\beta_j]} = f^{[\beta_j]}, \tag{2a}$$

$$\mathbf{q}^{[\beta_j]} = -\kappa^{[\beta_j]} \nabla T^{[\beta_j]}, \tag{2b}$$

$\rho^{[\beta_j]}$: mass density,

$c_{\mathrm{sp}}^{[\beta_j]}$: specific heat,

$T^{[\beta_j]}$: absolute temperature,

$\mathbf{q}^{[\beta_j]}$: heat flux,

$\kappa^{[\beta_j]}$: thermal conductivity,

$f^{[\beta_j]}$: power density of heat sources (induction heating).

Interface conditions

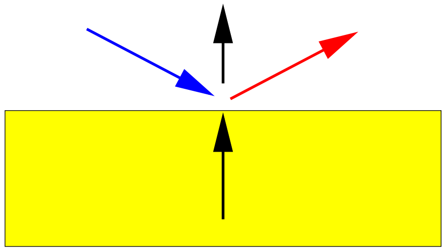

Continuity of the heat flux:

Between solid materials:

$$\left(\kappa^{[\beta]} \nabla T\right) \bullet \mathbf{n}^{[\beta]} = \left(\kappa^{[\beta']} \nabla T\right) \bullet \mathbf{n}^{[\beta]} \quad \text{on } \gamma_{\beta,\beta'}. \tag{1a}$$

Between gas and solid:

$$\left(\kappa^{(\mathrm{Ar})} \nabla T\right) \bullet \mathbf{n}_{\mathrm{gas}} \quad + R - J = \left(\kappa^{[\beta]} \nabla T\right) \bullet \mathbf{n}_{\mathrm{gas}} \quad \text{on } \gamma_{\beta,\mathrm{gas}}. \tag{1b}$$

$\mathbf{n}^{[\beta]}$: outer unit normal w.r.t. solid β, $\mathbf{n}_{\mathrm{gas}}$: outer unit normal w.r.t. gas phase,
R: radiosity, J: irradiation.

Continuity of temperature throughout apparatus.

Outer boundary conditions

Emission according to Stefan-Boltzmann law:

$$- \left(\kappa^{[\beta]} \nabla T\right) \bullet \mathbf{n}^{[\beta]} = \sigma \epsilon^{[\beta]}(T) \cdot \left(T^4 - T_{\mathrm{room}}^4\right), \quad (2)$$

ϵ: emissivity , σ: Boltzmann radiation constant,
$T_{\mathrm{room}} = 293$ K.

On surfaces of open cavities:

$$-(\kappa^{[\beta]} \nabla T) \bullet \mathbf{n}^{[\beta]} - R + J = 0. \quad (3)$$

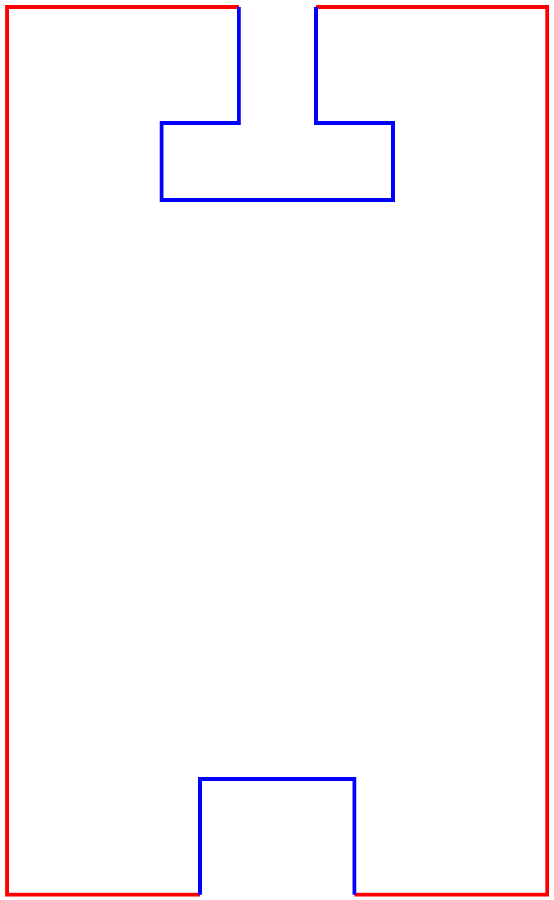

Overview

- SiC bulk single crystals: applications and growth process
- Modeling: balance equations, radiative heat transfer, induction heating
- Discretization: finite volume method
- Numerical simulation: software WIAS-HiTNIHS, transient simulation results
- Optimal control: theoretical results, numerical results

Model of diffuse-gray radiation

Goal: Compute $R - J$.

Assumption: Solid is opaque; reflection and emittance are independent of the angle of incidence and of the wavelength.

At each point of the surface Σ of the gas cavity:

$$R = E + J_{\mathrm{r}}, \tag{4}$$

E: emitted radiation, J_{r}: reflected radiation.

Stefan-Boltzmann law:

$$E(T) = \sigma\,\epsilon(T)\,T^4, \tag{5}$$

σ: Boltzmann radiation constant, ϵ: emissivity of the solid surface.

Opaqueness and Kirchhoff's law:

$$J_{\mathrm{r}} = (1 - \epsilon)\,J. \tag{6}$$

Model of diffuse-gray radiation (2)

Diffuseness yields:

$$J(T) = K(R(T)), \tag{7}$$

where

$$K(\rho)(x) := \int_\Sigma \Lambda(x,y)\,\omega(x,y)\,\rho(y)\,\mathrm{d}y \quad \text{(a.e. } x \in \Sigma\text{)}, \tag{8}$$

$$\Lambda(x,y) = \begin{cases} 1 & x \text{ and } y \text{ are mutually visible,} \\ 0 & \text{otherwise,} \end{cases} \tag{9}$$

$$\omega(x,y) := \frac{\big(\mathbf{n}_{\mathrm{g}}(y)\cdot(x-y)\big)\,\big(\mathbf{n}_{\mathrm{g}}(x)\cdot(y-x)\big)}{\pi\big((y-x)\cdot(y-x)\big)^2} \quad \big(\text{a.e. } (x,y)\in\Sigma^2,\ x\neq y\big). \tag{10}$$

Model of diffuse-gray radiation (3)

Combining (4) – (7) provides nonlocal equation for $R(T)$:

$$R(T) - \big(1 - \epsilon(T)\big)\, K(R(T)) = \sigma\, \epsilon(T)\, T^4. \tag{11}$$

One can write (11) in the form

$$G_T(R(T)) = E(T), \tag{12}$$

where the operator G_T is defined by

$$G_T(\rho) := \rho - \big(1 - \epsilon(T)\big)\, K(\rho). \tag{13}$$

Lemma: G_T is invertible. Thus:

$$R(T) = G_T^{-1}(E(T)). \tag{14}$$

Combining (11) and (7):

$$R(T) - J(T) = -\epsilon(T)\, \big(K(R(T)) - \sigma\, T^4\big). \tag{15}$$

Modeling Semi-Transparency

To model the semi-transparency of the SiC-crystal, a two band model is used, i.e. it is assumed that a range I_{refl} of wavelengths exists such that

- the crystal emits only lightwaves with wavelengths in I_{refl},
- lightwaves with wavelengths in I_{relf} are reflected or absorbed at the surface of the SiC–crystal,
- lightwaves with other wavelengths cross the crystal unaffected.

The contributions to the power density from I_{refl} and $\mathbb{R}^{+} \setminus I_{\mathrm{refl}}$ are then computed analogously to the opaque case.

Overview

- SiC bulk single crystals: applications and growth process
- Modeling: balance equations, radiative heat transfer, induction heating
- Discretization: finite volume method
- Numerical simulation: software WIAS-HiTNIHS, transient simulation results
- Optimal control: theoretical results, numerical results

Modeling induction heating

Assumptions:

- Cylindrical symmetry
- Sinusoidal time dependence
- No surface currents
- The gas phase is perfectly insulating
- All solids are possibly conducting materials
- Given total voltage in the induction coil:

$$V(t) = V_0 \sin(\omega t).$$

Heating mechanism:

alternating voltage $\Rightarrow$ alternating current

$\Rightarrow$ alternating magnetic field

$\Rightarrow$ eddy currents

$\Rightarrow$ heat sources (Joule effect)

Goal: Computation of heat source distribution

Voltage inside coil rings:

- Replace coil by N axisymmetric rings
- Voltage in the k-th ring: $v_k(t) = \mathrm{Im}(\mathbf{v}_k e^{i\omega t})$.
- Decomposition of total voltage:

$$\sum_{k=1}^{N} \mathbf{v}_k = V_0. \tag{9}$$

Heat sources:

$$\mu(r,z) = \frac{|\mathbf{j}(r,z)|^2}{2\,\sigma(r,z)}, \tag{10}$$

μ: power density (per volume) of heat sources,

$\mathbf{j}$: current density,

σ: electrical conductivity,

(r,z): cylindrical coordinates.

Magnetic scalar potential:

There exists a complex-valued magnetic scalar potential ϕ such that

$$\mathbf{j} = \begin{cases} -i\omega\,\sigma\,\phi + \frac{\sigma\,\mathbf{v}_k}{2\pi r} & \text{(inside } k\text{-th ring),} \\ -i\omega\,\sigma\,\phi & \text{(other conductors).} \end{cases} \tag{11}$$

Elliptic system of PDEs for ϕ:

- In insulators:

$$-\nu\,\mathrm{div}\,\frac{\nabla(r\phi)}{r^2} = 0. \tag{12a}$$

- In the k-th coil ring:

$$-\nu\,\mathrm{div}\,\frac{\nabla(r\phi)}{r^2} + \frac{i\,\omega\sigma\phi}{r} = \frac{\sigma\,\mathbf{v}_k}{2\pi r^2}. \tag{12b}$$

- In other conductors:

$$-\nu\,\mathrm{div}\,\frac{\nabla(r\phi)}{r^2} + \frac{i\,\omega\sigma\phi}{r} = 0. \tag{12c}$$

- Interface condition: Between $\mathrm{material}_1$ and $\mathrm{material}_2$:

$$\left(\frac{\nu_{\mathrm{material}_1}}{r^2}\nabla(r\phi)_{\mathrm{material}_1}\right)\bullet\mathbf{n}_{\mathrm{material}_1} = \left(\frac{\nu_{\mathrm{material}_2}}{r^2}\nabla(r\phi)_{\mathrm{material}_2}\right)\bullet\mathbf{n}_{\mathrm{material}_1}. \tag{12d}$$

- Outer boundary condition:

$$\phi = 0. \tag{12e}$$

- ϕ is assumed to be continuous everywhere.

ν: magnetic reluctivity,

$\mathbf{n}_{\mathrm{material}_1}$: outer unit normal w.r.t. $\mathrm{material}_1$.

Current inside coil rings:

For each solution ϕ of (12), the corresponding total current inside the k-th coil ring is

$$\mathbf{j}_k(\mathbf{v}_k, \phi) = \frac{\mathbf{v}_k}{2\pi} \int_{\Omega_k} \frac{\sigma}{r} \, \mathrm{d}r\mathrm{d}z \, - i\omega \int_{\Omega_k} \sigma\phi \, \mathrm{d}r\mathrm{d}z \, , \tag{13}$$

Ω_k: domain of (circular) 2d-projection of the k-th coil ring.

Equal total current in each ring:

- As the rings must approximate a single connected coil:

$$\mathbf{j}_k(\mathbf{v}_k, \phi) = \mathbf{j}_{k+1}(\mathbf{v}_{k+1}, \phi), \quad k \in \{1, \dots, N-1\}. \tag{14}$$

  The $\mathbf{v}_k$ must satisfy the linear system consisting of (9) and (12) – (14).

- Scaling of solution $(\phi, \mathbf{v}_1, \dots, \mathbf{v}_N)$ admits prescribing the total power.

Overview

- SiC bulk single crystals: applications and growth process
- Modeling: balance equations, radiative heat transfer, induction heating
- Discretization: finite volume method
- Numerical simulation: software WIAS-HiTNIHS, transient simulation results
- Optimal control: theoretical results, numerical results

Discretization of heat equation: finite volume method

Recall form of heat equation for T:

$$\frac{\partial \varepsilon_m(T,x)}{\partial t} - \operatorname{div}\big(\kappa_m(T)\,\nabla T\big) - f_m(T,t,x) = 0 \quad \text{on } [0,t_{\mathrm{f}}] \times \Omega_m.$$

Time discretization by implicit Euler scheme:

$0 = t_0 < \cdots < t_N = t_{\mathrm{f}},\ N \in \mathbb{N},$

$k_n := t_n - t_{n-1},$

$\Delta := \max\{k_n :\ n = 1, \ldots, N\}.$

Space discretization: $\Omega := \bigcup_m \Omega_m$ is discretized into control volumes using a constraint Delaunay triangulation.

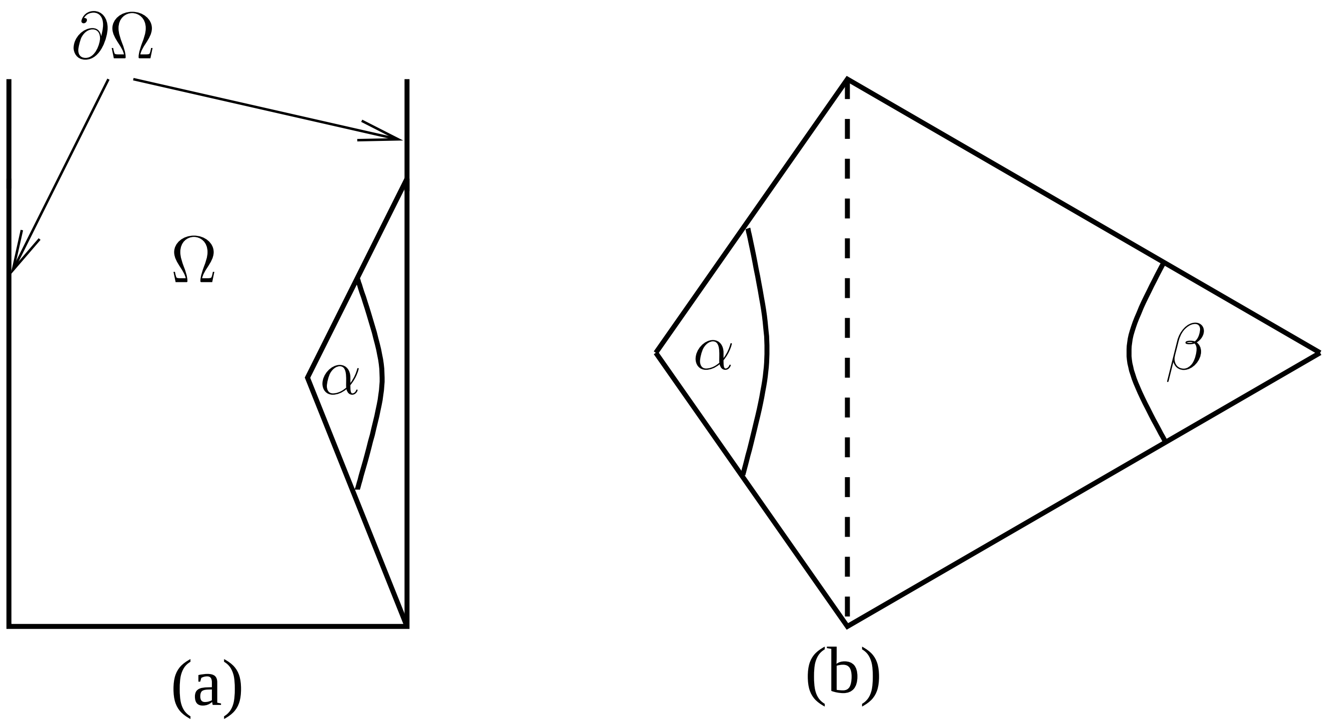

Figure 1: (a): Violates constrained Delaunay criterion. (b): Violates constrained Delaunay criterion if and only if dashed line constitutes not only a common edge of two triangles, but also an interface between different domains Ω_{m_1} and Ω_{m_2}.

Let V denote the set of vertices of the constraint Delaunay triangulation. For each $v \in V$ define the Voronoï box centered at v:

$$\omega_v := \overline{\left\{x \in \Omega : \|x - v\|_2 < \|x - w\|_2 \text{ for each } w \in V \setminus \{v\}\right\}}.$$

For each m, v: $\omega_{m,v} := \omega_v \cap \Omega_m$.

Then: $\Omega_m = \bigcup_{v \in V_m} \omega_{m,v}$, where $V_m := V \cap \Omega_m$,

Notation: λ_2 and λ_1: 2-dimensional and 1-dimensional Lebesgue measure,

$\mathrm{nb}_m(v) := \{w \in V_m \setminus \{v\} : \lambda_1(\omega_{m,v} \cap \omega_{m,w}) \neq 0\}$: set of m-neighbors of v.

Finite volume scheeme in cylindrical coordinates:

Find nonnegative solution $(\mathbf{T}_0, \ldots, \mathbf{T}_N)$, $\mathbf{T}_n = (T_{n,v})_{v \in V_\Omega}$, to

$$
\begin{aligned}
T_{0,v} &= T_{\text{room}} && (v \in V_\Omega), \\
\mathcal{H}_{n,v}(\mathbf{T}_{n-1}, \mathbf{T}_n) &= 0 && (v \in V_\Omega, \quad n \in \{1, \ldots, n\}),
\end{aligned}
$$

where for each $n \in \{1, \ldots, n\}$:

$$
\begin{aligned}
&\mathcal{H}_{n,v}(\mathbf{T}_{n-1}, \mathbf{T}_n) \\
&:= k_n^{-1} \sum_m \big(\varepsilon_m(T_{n,v}, v) - \varepsilon_m(T_{n-1,v}, v)\big) \cdot v_r \cdot \lambda_2(\omega_{m,v}) \\
&\quad - \sum_m \sum_{w \in \text{nb}_m(v)} \frac{\kappa_m(T_{n,v}) \cdot v_r + \kappa_m(T_{n,w}) \cdot w_r}{2} \cdot \frac{T_{n,w} - T_{n,v}}{\|v - w\|_2} \cdot \lambda_1\big(\omega_{m,v} \cap \omega_{m,w}\big) \\
&\quad + \sum_m \sigma\, \epsilon_m(T_{n,v}) \cdot (T_{n,v}^4 - T_{\text{room}}^4) \cdot v_r \cdot \lambda_1(\partial\omega_{m,v} \cap \partial\Omega) \\
&\quad - \sum_m f_m(T_{n,v}, t_n, v) \cdot v_r \cdot \lambda_2(\omega_{m,v}).
\end{aligned}
$$

Theorem:

Assume (i) – (iv):

(i) $\varepsilon_m \geq 0$, $\kappa_m \geq 0$, $\epsilon_m \geq 0$, and $f(0,t,x) \geq 0$.

(ii) $\varepsilon_m(\cdot, x)$ is increasing, and there is $L > 0$ such that
$|\varepsilon_m(T,x) - \varepsilon_m(\tilde{T},x)| \geq L\,|T - \tilde{T}|$ for each $x \in \Omega_m$.

(iii) κ_m, ϵ_m, and f_m are locally Lipschitz in their T-dependence.

(iv) f_m is bounded from above.

Then there is $M > 0$ (independent of the time discretization) and Δ_M such that, for $\Delta < \Delta_M$, the finite volume scheme has a unique solution
$(\mathbf{T}_0, \dots, \mathbf{T}_N) \in \left([0,M]^{V_\Omega}\right)^{N+1}$.

Overview

- SiC bulk single crystals: applications and growth process
- Modeling: balance equations, radiative heat transfer, induction heating
- Discretization: finite volume method
- Numerical simulation: software WIAS-HiTNIHS, transient simulation results
- Optimal control: theoretical results, numerical results

The software WIAS-HiTNIHS

(High Temperature Numerical Induction Heating Simulator)

Developers: Jürgen Geiser, Olaf Klein (WIAS)
Christian Meyer (TU Berlin)
Peter Philip (IMA)

Cooperation with: Institute of Crystal Growth (IKZ) Berlin

Purpose:

- Transient simulation of induction-heated systems
- Systematic study and optimization of control parameters such as
  - Geometrical setup of apparatus
  - Positioning of induction coil
  - Heating power

Simulated phenomena

- Axisymmetric heat source distribution
  - Sinusoidal alternating voltage
  - Correct voltage distribution to the coil rings
  - Temperature-dependent electrical conductivity
- Axisymmetric temperature distribution
  - Heat conduction through gas phase and solid components of growth apparatus
  - Non-local radiative heat transport between surfaces of cavities
  - Radiative heat transport through semi-transparent materials
  - Convective heat transport

Numerical models and methods

- Induction heating:
  - Determination of complex scalar magnetic potential from elliptic partial differential equation
  - Calculation of heat sources from potential
- Temperature field:
  - View factor calculation
  - Band model of semi-transparency
  - Solution of parabolic partial differential equation

Discretization and implementation

- Implicit Euler method in time
- Finite volume method in space
  - Constraint Delaunay triangulation of domain yields Voronoï cells
  - Full upwinding for convection terms
  - Complicated nonlinear system of equations
  - Solution by Newton's method
- Implementation tools:
  - Program package pdelib
  - Grid generator Triangle
  - Matrix solver Pardiso

Overview

- SiC bulk single crystals: applications and growth process
- Modeling: balance equations, radiative heat transfer, induction heating
- Discretization: finite volume method
- Numerical simulation: software WIAS-HiTNIHS, transient simulation results
- Optimal control: theoretical results, numerical results

Computed temperature differences between top and bottom: $P_{\max} = 7$ kW

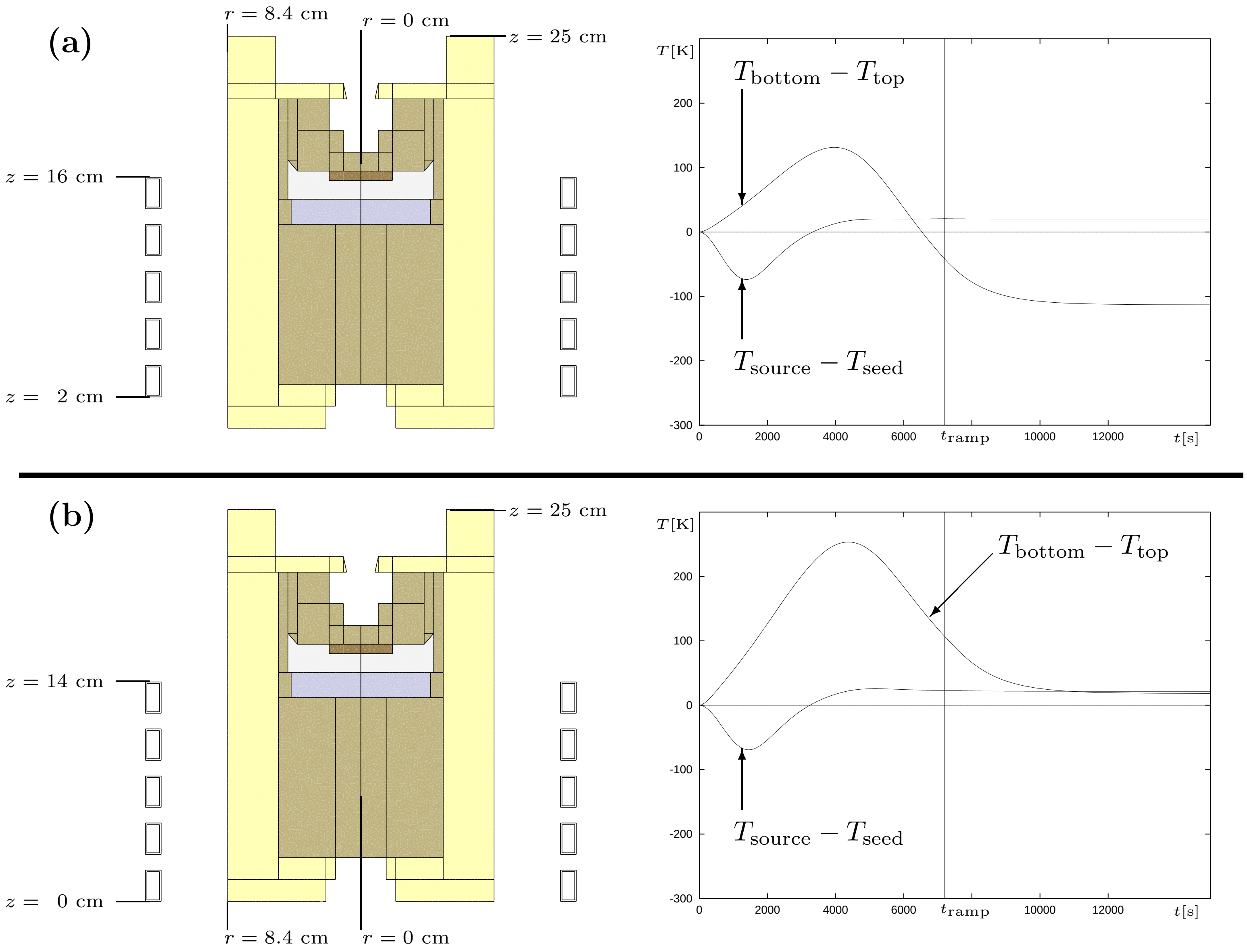

Computed temperature differences between top and bottom: $P_{\max} = 5.5/8.5$ kW

(lower coil position in both cases)

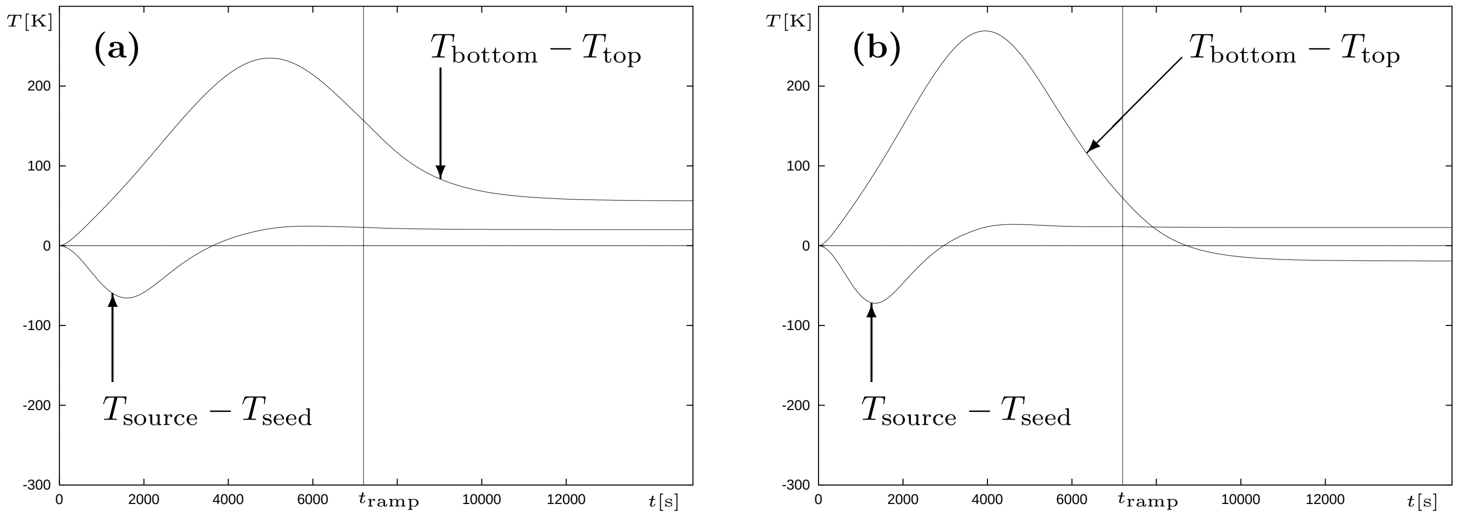

Computed temperature evolution of the powder charge: $P_{\max} = 7$ kW

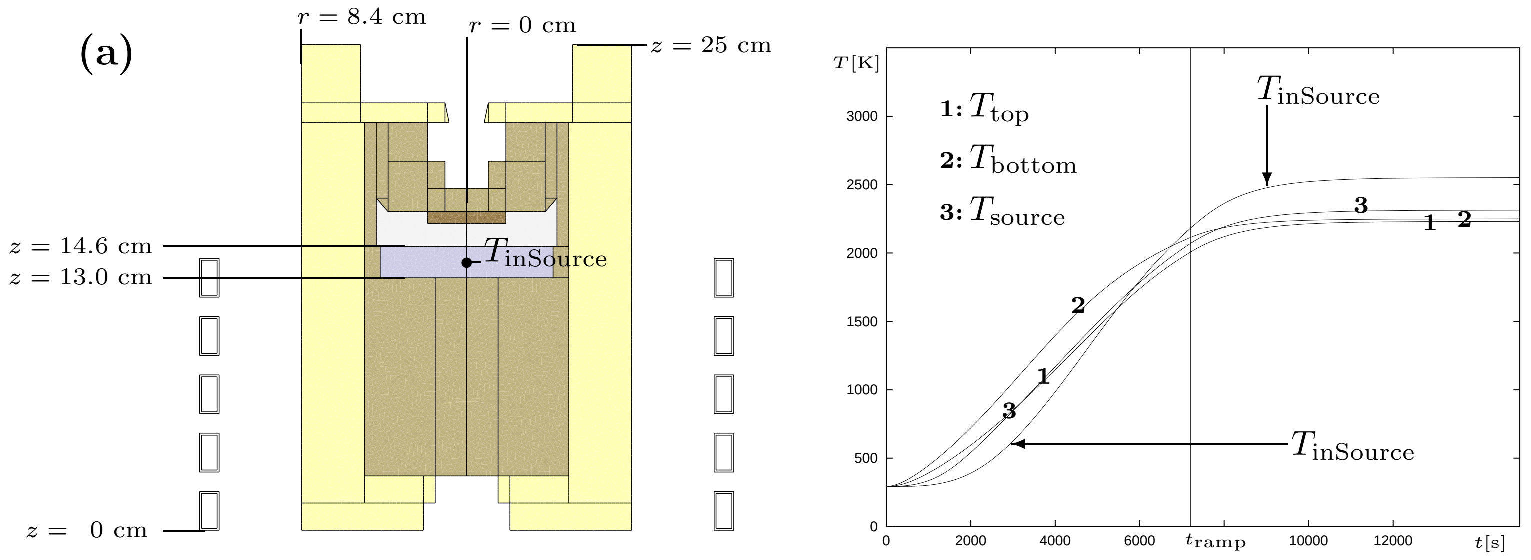

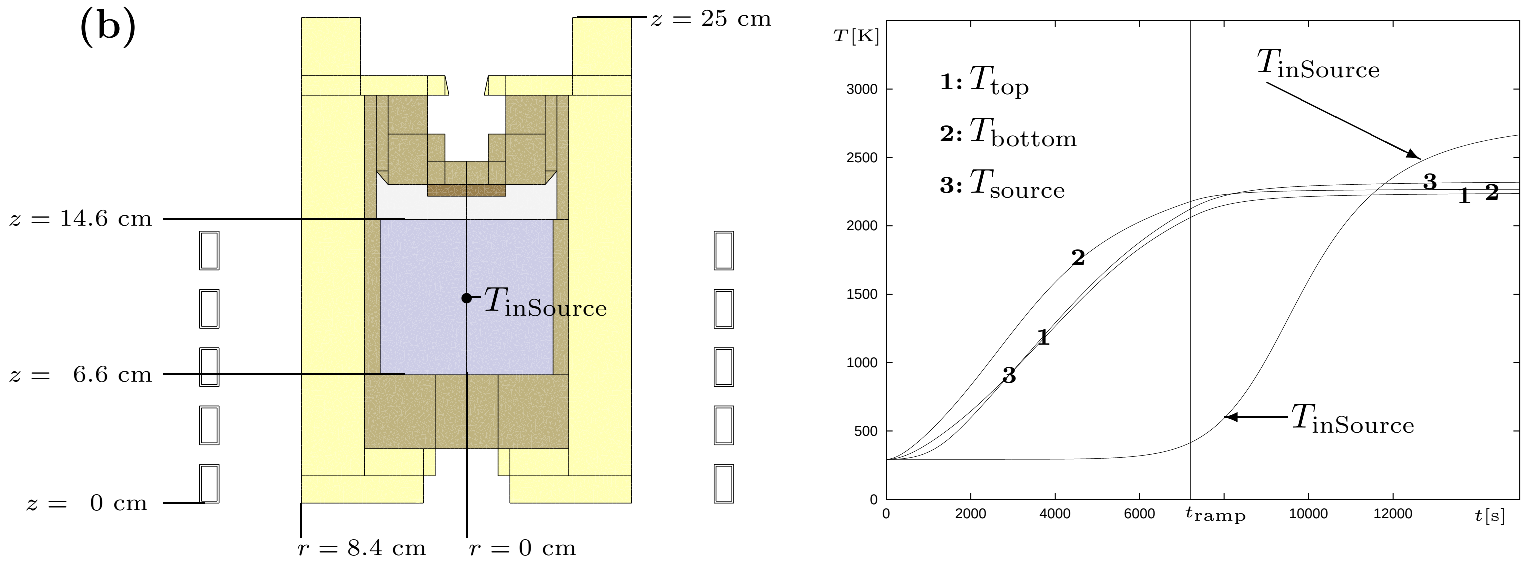

Overview

- SiC bulk single crystals: applications and growth process
- Modeling: balance equations, radiative heat transfer, induction heating
- Discretization: finite volume method
- Numerical simulation: software WIAS-HiTNIHS, transient simulation results
- Optimal control: theoretical results, numerical results

Aims of the project

Improving the crystal's growth by controlling suitable parameters to reach a desired temperature profile

But: Complete problem is too complex for theoretic analysis.

⇒ **Two-fold strategy**:

1. Mathematical analysis for a simplified model
2. Numerical optimization of a comprehensive model relevant to application

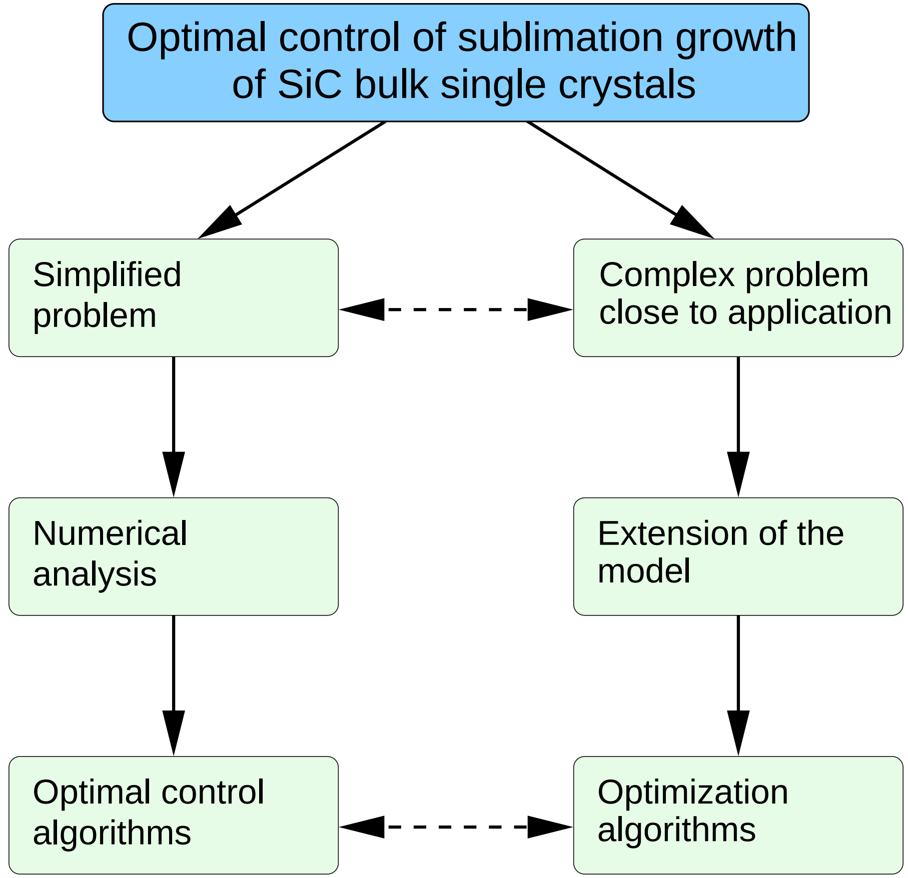

Simplified model

Optimal control problem for the heat equation with non-local radiation boundary conditions:

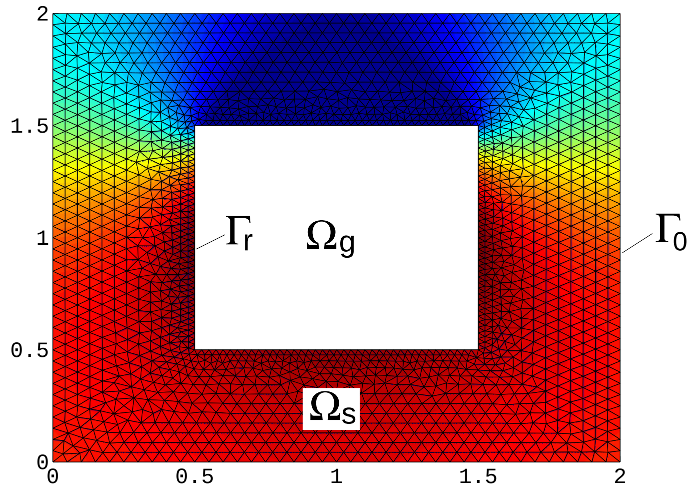

minimize $\displaystyle \frac{1}{2}\int_{\Omega_g} |\nabla y - z|^2\,dx + \frac{\nu}{2}\int_{\Omega_s} u^2\,dx$

subject to

$$-\text{div}(\kappa\,\nabla y) = u \quad \text{in } \Omega$$

$$\kappa_g \left(\frac{\partial y}{\partial n_r}\right)_g - \kappa_s \left(\frac{\partial y}{\partial n_r}\right)_s = G(\sigma|y|^3 y) \quad \text{on } \Gamma_r$$

$$\kappa_s \frac{\partial y}{\partial n_0} = \varepsilon\sigma(y_a^4 - |y|^3 y) \quad \text{on } \Gamma_0$$

(G: non-local radiation operator)

- Existence of an optimal solution and necessary optimality conditions in the semilinear case with pointwise control constraints
- Regularization technique for the linear case with pointwise state constraints

Stationary optimal control problem for the temperature field

Known fact: Crystal surface forms along isotherms.

Goal: Radially constant isotherms during growth.

Control: $\int_{\Omega_{\text{gas}}} w(z)\left(\frac{\partial T}{\partial r}(r,z)\right)^2 \mathrm{d}(r,z) \longrightarrow \min.$

PDEs ($\mathbf{v}_{\text{gas}} = 0$, $f(x,T,P) = f(x,P)$):

$$-\operatorname{div}\left(\kappa^{(\text{Ar})}(T)\,\nabla T\right) = 0 \quad \text{in } \Omega_{\text{gas}},$$

$$-\operatorname{div}\left(\kappa(x,T)\,\nabla T\right) = f(x,P) \quad \text{in } \Omega \setminus \Omega_{\text{gas}}.$$

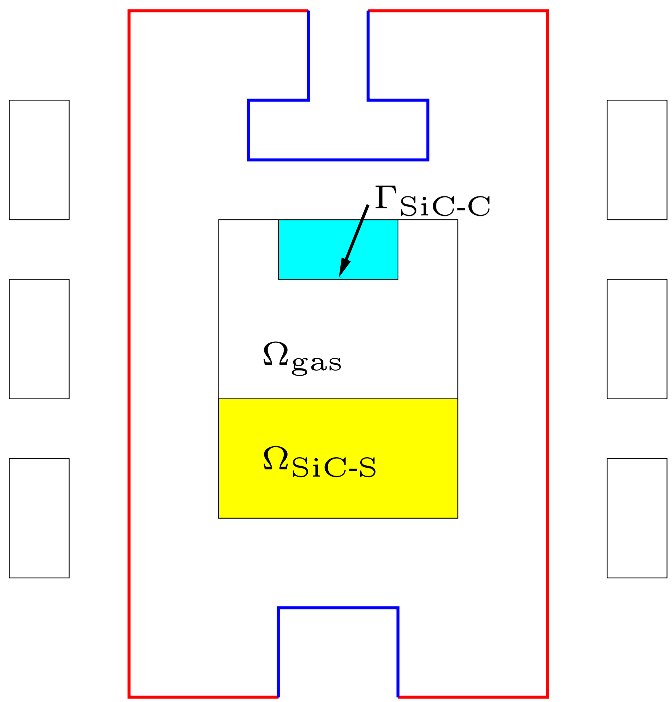

Constraints:

- $T_{\text{room}} \le T \le T_{\max}$ in Ω,
- $T_{\min,\text{SiC-C}} \le T \le T_{\max,\text{SiC-C}}$ on $\Gamma_{\text{SiC-C}}$ (need right polytype),
- $T|_{\Omega_{\text{SiC-S}}} \ge T|_{\Gamma_{\text{SiC-C}}} + \delta$, $\delta > 0$ (source temp. $\ge$ seed temp. $+\delta$),
- $0 \le P \le P_{\max}$ (bounds for heating power P (control parameter)).

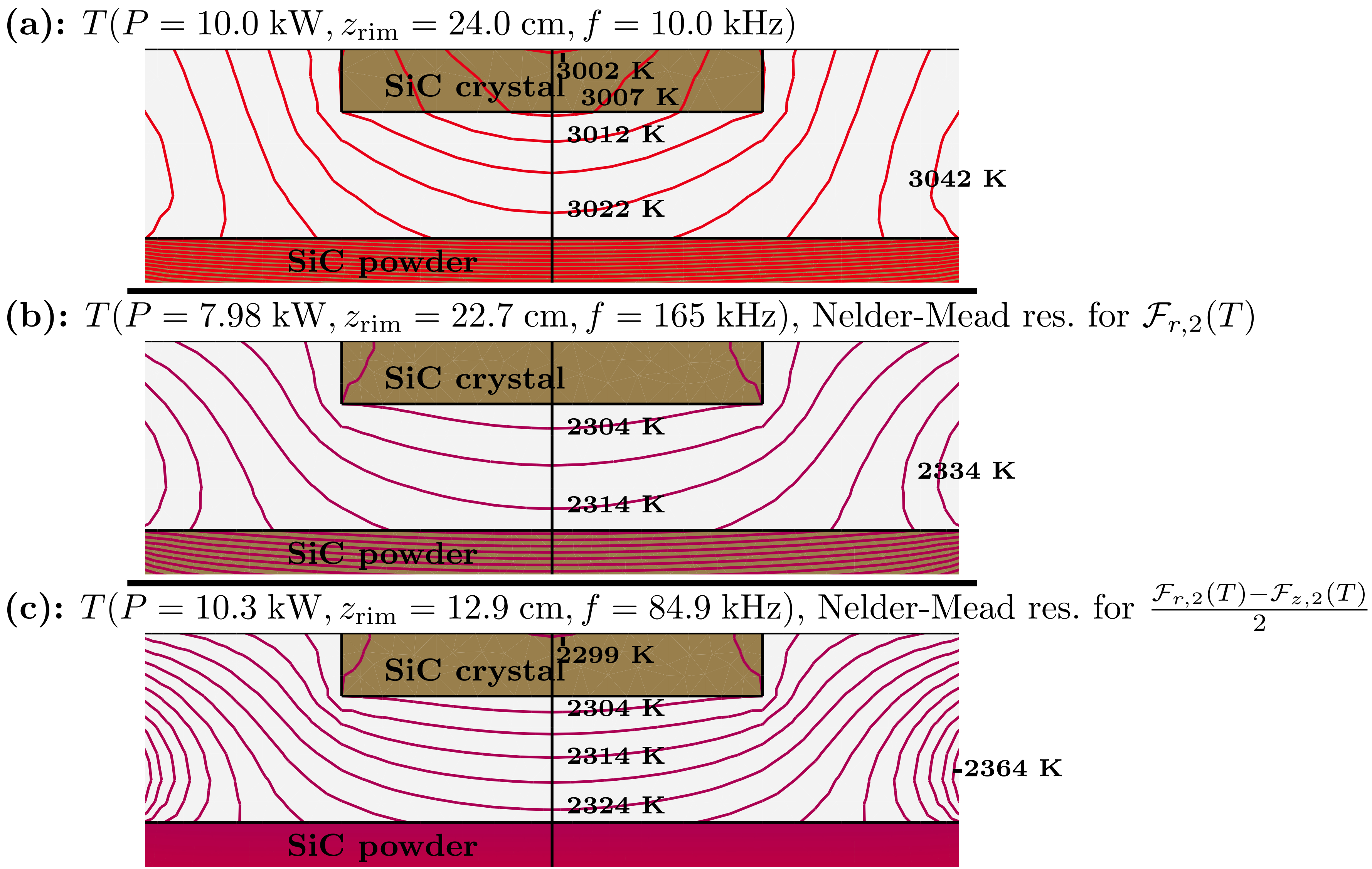

(a): $T(P = 10.0\text{ kW}, z_{\text{rim}} = 24.0\text{ cm}, f = 10.0\text{ kHz})$
SiC crystal
3002 K
3007 K
3012 K
3022 K
3042 K
SiC powder
(b): $T(P = 7.98\text{ kW}, z_{\text{rim}} = 22.7\text{ cm}, f = 165\text{ kHz})$, Nelder-Mead res. for $\mathcal{F}_{r,2}(T)$
SiC crystal
2304 K
2314 K
2334 K
SiC powder
(c): $T(P = 10.3\text{ kW}, z_{\text{rim}} = 12.9\text{ cm}, f = 84.9\text{ kHz})$, Nelder-Mead res. for $\frac{\mathcal{F}_{r,2}(T) - \mathcal{F}_{z,2}(T)}{2}$
SiC crystal
2299 K
2304 K
2314 K
2324 K
2364 K
SiC powder

Thank You for Your Attention !

Once Again: Publications / More Information:

`http://www.ima.umn.edu/~philip/sic/#Publications`

`http://www.ima.umn.edu/~philip/sic/`